Uniform Coverage Control of Mobile Sensor Networks for Dynamic Target Detection

George Mathew, Amit Surana and Igor Mezić

Abstract— **In surveillance problems, the uncertainty in the position of a target can be specified in terms of a probability distribution. To reduce the average search times to detect a target using mobile sensors, it is desirable to have the trajectories of the sensors sample the probability distribution uniformly. When the target is moving, the initial uncertainty in the position of the target evolves forward in time according to the target dynamics. We assume a model for the dynamics of the target and build upon our previous work for stationary targets to define appropriate metrics for uniform coverage of the evolving probability distribution. Using these metrics, we derive centralized feedback control laws for the motion of the sensors so that they achieve uniform coverage of the moving target distribution. We demonstrate the performance of the algorithm on various scenarios.**

I. Introduction

Cooperative control of mobile robotic/sensor networks is an emerging discipline with a lot of recent research activity. This is partly due to the various technological advances in robotic/sensor networks, and partly due to the interesting mathematical challenges that arise from cooperative control problems. For working prototypes of mobile sensor networks see [1] and [2]. The emergence of cooperative control as a discipline can be affirmed by special journal issues dedicated entirely to various problems in cooperative control. See [3] and [4] for special issues presenting papers that deal with a wide range of coordination tasks such as consensus, connectivity maintenance, formation stabilization, coverage and target detection. See [5] for a special issue dedicated to coordinated control of multiple mobile, networked sensor platforms for ocean state estimation.

In this paper, we address the problem of coverage of moving targets by multiple mobile sensors. Some representative papers that deal with the problem of coverage/sampling are [6], [7],[8], [9] and [10]. In our recent work ([11] and [12]), we proposed an algorithm so that points on the trajectories of the mobile sensors uniformly sample a stationary probability distribution. Such an algorithm is useful when there is uncertainty in the position of a stationary target that needs to be detected. The uncertainty in the position of the target can be specified in terms of a probability distribution. To reduce the average search times to detect the target, it is desirable that the sensor trajectories uniformly sample this probability distribution. In [11] and [12], we borrowed concepts from ergodic theory to define appropriate metrics for uniformity of coverage, and designed centralized feedback control laws to achieve uniform coverage. In this paper, we extend the work in [11] and [12], to define appropriate metrics for uniform coverage when there is uncertainty in the position of a moving target.

A system is said to exhibit *ergodic dynamics* if it visits every subset of the phase space with a probability equal to the *measure* of that subset. For good coverage of a stationary target, this translates to requiring that the amount of time spent by the mobile sensors in an arbitrary set be proportional to the probability of finding the target in that set. For good coverage of a dynamic target, this translates to requiring that the amount of time spent in certain 'tube sets' be proportional to the probability of finding the target in the "tube sets". We assume a model for the motion of the targets to construct these "tube sets" and define appropriate metrics for coverage. (The model for the target motion can be approximate and the dynamics of targets for which we don't have precise knowledge can be captured using stochastic models). Using this metric of coverage, we derive centralized feedback control laws for the motion of the mobile sensors. The algorithm proposed in this paper will be referred to as Dynamic Spectral Multiscale Coverage (DSMC).

There are many applications of mobile multi-sensor systems where it is useful to design their dynamics so that they uniformly sample an evolving probability distribution. A couple of such scenarios are

1) **Ocean Monitoring:** Autonomous ocean-sampling networks is an active area of research, see for examples [1], [5] and [9]. The central objective in these projects is to collect data that best reveals the ocean processes and dynamics. They use fleets of underwater gliders in the ocean that take measurements of various oceanographic fields like temperature, salinity and the flow. The algorithm proposed in this paper can be used to uniformly sample a moving domain advected by the ocean flow or to detect a moving target like a submarine whose position is uncertain.
2) **Target search and tracking:** For military applications and search-and-rescue operations, detection of moving targets using audio/video signals is an important task. For such tasks, it is desirable that the trajectories of the mobile sensors are such that it is difficult for a target to evade detection by the sensors. Of particular interest is the problem of minimizing the time for target detection when the sensor range is very small compared to the

George Mathew is with the United Technologies Research Center, Inc., Berkeley, CA mathewga@utrc.utc.com

Amit Surana is with the United Technologies Research Center, East Hartford, CT SuranaA@utrc.utc.com

Igor Mezić is with the Department of Mechanical Engineering at the University of California, Santa Barbara mezic@engineering.ucsb.edu

domain size, and when there is uncertainty in the terrain and sensor measurements.

The rest of the paper is structured as follows. In Section II, we present the metric that quantifies how well a set of trajectories sample a evolving probability distribution. In Section III, we use this metric to design dynamics (or feedback control) for multiple sensors that move according to either first-order dynamics or second-order dynamics. We numerically analyze the behavior of the closed-loop dynamics for various scenarios. In Section IV, we describe the case where the target dynamics is uncertain. In Section V, we apply the DSMC algorithm for deterministic target dynamics and also consider a case when the uncertainty in the position of the target is updated using a Kalman filter.

II. Problem Setup

First, we discuss the coverage problem when the target dynamics is first-order and deterministic. In section IV, we will extend this framework to account for uncertainty in target dynamics. Let the target motion model be described by a deterministic set of ODE's

$$\dot{z}(t) = v(z(t),t), \tag{1}$$

where, $z(t) \in U$, $U \subset \mathbb{R}^2$ being the region in which the target motion is confined to over a period $[0,T_f]$ of interest. Let T be the corresponding mapping that describes the evolution of the target position. i.e., if the target is at point $z(t_0)$ at time $t = t_0$, its position at time $t = t_f$ is given by

$$z(t_f) = T(z(t_0),t_0,t_f). \tag{2}$$

Given a set $A \subset U$ its inverse image under the transformation $T(.,t_0,t_f)$ is given as

$$T^{-1}(.,t_0,t_f)(A) = \{y : T(y,t_0,t_f) \in A\}. \tag{3}$$

The initial uncertainty in the position of the target is specified by the probability distribution $\mu(0,x) = \mu_0(x)$. The uncertainty in the position of the target evolves according to

$$\mu(t,A) = \int_A \mu(t,y)dy = \int_{T^{-1}(.,0,t)(A)} \mu_0(y)dy. \tag{4}$$

Throughout the paper, we use the notation such that $\mu(t,A)$ will denote the probability measure of the set A.

Let $[P^{t_0,t_f}]$ be the family of Perron-Frobenius operators corresponding to the transformations $T(.,t_0,t_f)$. i.e.,

$$\int_A [P^{t_0,t_f}]\mu(t_0,y)dy = \int_A \mu(t_f,y)dy = \int_{T^{-1}(.,t_0,t_f)(A)} \mu(t_0,y)dy. \tag{5}$$

In particular, we have

$$\int_A [P^{0,t}]\mu_0(y)dy = \int_A \mu(t,y)dy. \tag{6}$$

At time t, consider the spherical set $B(x,r)$ with radius r and center at x. Now consider the corresponding tube set given as

$$H^t(B(x,r)) = \{(y,\tau) : \tau \in [0,t] \text{ and } T(y,\tau,t) \in B(x,r)\}. \tag{7}$$

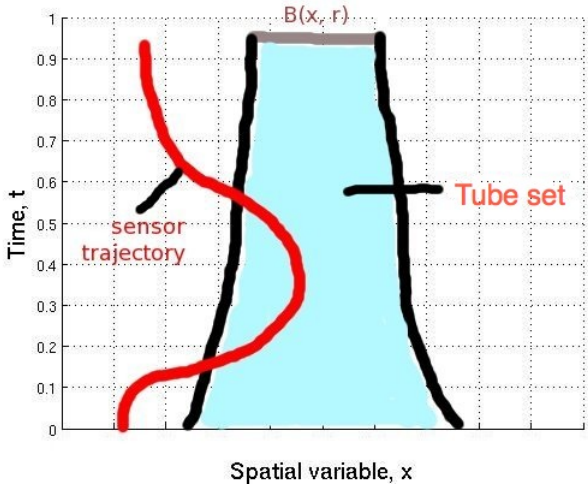

Fig. 1. The tube set $H^t(B(x,r))$ is a subset of the extended space-time domain and is the union of the sets $T^{-1}(.,\tau,t)(B(x,r)) \times \{\tau\}$ for all $\tau \in [0,t]$. Note that there is no particular reason that the target trajectories going back in time should diverge. They could just as well converge and then the set of initial target conditions leading to $B(x,r)$ could get smaller and smaller. This still does not change the observation in (8).

The tube set $H^t(B(x,r))$ (See Figure 1) is a subset of the extended space-time domain and is the union of the sets $T^{-1}(.,\tau,t)(B(x,r)) \times \{\tau\}$ for all $\tau \in [0,t]$. This tube set can be thought of as the set of all points in the extended space-time domain that end up in the spherical set $B(x,r)$ at time t when evolved forward in time according to the target dynamics. Note that the probability of finding a target within any time slice of the tube set is the same. i.e.,

$$\begin{aligned} \mu(\tau_1, T^{-1}(.,\tau_1,t)(B(x,r))) &= \mu(\tau_2, T^{-1}(.,\tau_2,t)(B(x,r))) \\ &= \mu(t, B(x,r)), \\ &\text{for all } \tau_1,\tau_2 \le t. \end{aligned} \tag{8}$$

This is because none of the possible target trajectories either leave or enter the tube set $H^t(B(x,r))$. Let the sensor trajectories be $x_j : [0,t] \to \mathbb{R}^2$ for $j = 1,2,..,N$. The fraction of the time spent by the sensor trajectories $(x_j(t),t)$ in the tube set $H^t(B(x,r))$ is given as

$$\begin{aligned} d^t(x,r) &= \frac{1}{Nt}\sum_{j=1}^{N}\int_0^t \chi_{T^{-1}(.,\tau,t)(B(x,r))}(x_j(\tau))\,d\tau \\ &= \frac{1}{Nt}\sum_{j=1}^{N}\int_0^t \chi_{B(x,r)}(T(x_j(\tau),\tau,t))\,d\tau. \end{aligned} \tag{9}$$

$\chi_{B(x,r)}$ is the indicator function on the set $B(x,r)$. It might appear that the fraction $d^t(x,r)$ is hard to compute. But it turns out that this fraction can be computed as the spherical integral

$$d^t(x,r) = \int_{B(x,r)} C^t(y)dy, \tag{10}$$

of a distribution,

$$C^t(x) = \frac{1}{Nt}\sum_{j=1}^{N}\int_0^t P^{\tau,t}\delta_{x_j(\tau)}(x)d\tau, \tag{11}$$

which we refer to as the *coverage distribution*. Here δ_{x_0} is the delta distribution with mass at the point x_0. The *coverage distribution* C^t can be thought of as the distribution of points visited by the mobile sensors when evolved forward in time according to the target dynamics. To see that the expression in (10) is equal to the expression in (9), observe that

$$\begin{aligned} d^t(x,r) &= \int\limits_{B(x,r)} C^t(y)dy = \int\limits_{B(x,r)}\left[\frac{1}{Nt}\sum_{j=1}^{N}\int_0^t P^{\tau,t}\delta_{x_j(\tau)}(y)d\tau\right]dy \\ &= \frac{1}{Nt}\sum_{j=1}^{N}\int_0^t\left[\int\limits_{B(x,r)} P^{\tau,t}\delta_{x_j(\tau)}(y)dy\right]d\tau \\ &= \frac{1}{Nt}\sum_{j=1}^{N}\int_0^t\left[\int\limits_{T^{-1}(.,\tau,t)(B(x,r))}\delta_{x_j(\tau)}(y)dy\right]d\tau \\ &= \frac{1}{Nt}\sum_{j=1}^{N}\int_0^t \chi_{T^{-1}(.,\tau,t)(B(x,r))}\left(x_j(\tau)\right)d\tau. \end{aligned} \tag{12}$$

In Appendix B we describe a iterative procedure to numerically compute an approximation to the coverage distribution C^t.

For certain applications (e.g. uniform sampling), it is desirable that the fraction of the time spent by the sensor trajectories in the tube set must be close to

$$\mu(t,B(x,r)) = \int\limits_{B(x,r)}\mu(t,y)dy = \int\limits_{T^{-1}(.,0,t)(B(x,r))}\mu_0(y)dy. \tag{13}$$

For such problems, we can use the metric

$$E^2(t) = \int_0^R\int\limits_U\left(C^t(B(x,r)) - \mu(t,B(x,r))\right)^2 dxdr, \tag{14}$$

For search and tracking problems, the above metric can be generalized to

$$E^2(t) = \int_0^R\int\limits_U\left(C^t(B(x,r)) - \nu(t,B(x,r))\right)^2 dxdr. \tag{15}$$

where,

$$\nu(t,x) = \mathscr{F}(t,\mu(t,x))/\int_U \mathscr{F}(t,\mu(t,x))dx. \tag{16}$$

is a function of μ. For e.g. in search problems where it is desirable that the sensors spend more time in regions where there is higher uncertainty in the target position, $\mathscr{F}$ can be taken to be

$$\mathscr{F}(t,\mu(t,x)) = -\mu(t,x)\log\mu(t,x). \tag{17}$$

The metric $E(t)$ essentially compares the spherical integrals of the distributions C^t and $\nu(t,.)$. As described in [11], [12] and [13], $E(t)$ is equivalent to a metric induced by a Sobolev space norm of negative index $s = (n+1)/2$. i.e.,

$$c_1\|C^t - \nu(t,.)\|_{H^{-s}}^2 \leq E^2(t) \leq c_2\|C^t - \nu(t,.)\|_{H^{-s}}^2. \tag{18}$$

The Sobolev space distance can also be expressed as

$$\begin{aligned} \phi^2(t) = \|C^t - \nu(t,.)\|_{H^{-s}}^2 &= \sum_{K\in\mathbb{Z}^{*n}}\Lambda_k|s_k(t)|^2, \\ \text{where } s_k(t) = c_k(t) - \nu_k(t), \quad \Lambda_k &= \frac{1}{(1+\|k\|^2)^s} \\ c_k(t) = \left\langle C^t, f_k\right\rangle &\text{ and } \nu_k(t) = \left\langle \nu(t,.), f_k\right\rangle. \end{aligned} \tag{19}$$

Here $\{f_k\}$ are the Fourier basis functions that satisfy Neumann boundary conditions on the rectangular domain U and k is the corresponding wave-number vector. For instance, on a rectangular domain $U = [0,L_1]\times[0,L_2]$, we have,

$$\begin{aligned} f_k(x) &= \frac{1}{h_k}cos(k_1x_1)cos(k_2x_2), \text{where} \\ k_1 &= \frac{K_1\pi}{L_1} \text{ and } k_2 = \frac{K_2\pi}{L_2}, \\ &\text{for } K_1, K_2 = 0,1,2.... \text{ and where} \\ h_k &= \left(\int_0^{L_1}\int_0^{L_2} cos^2(k_1x_1)cos^2(k_2x_2)dx_1dx_2\right)^{1/2}, \end{aligned} \tag{20}$$

is a normalization constant.

III. Feedback Control Design

Assume that there are N mobile sensors which evolve either by first-order or second-order dynamics. First-order dynamics is described by

$$\dot{x}_j(t) = u_j(t). \tag{21}$$

For convenience, let us define the quantity

$$\begin{aligned} \Phi(t) = \frac{1}{2}N^2t^2\phi^2(t) &= \frac{1}{2}\sum_K\Lambda_k|S_k(t)|^2 \\ \text{where } S_k(t) &= Nts_k(t). \end{aligned} \tag{22}$$

At any given time t, we consider the following optimal control problem over the time horizon $[t,t+\Delta t]$. With the aim to drive the sensors to positions which lead to the highest rate of decay of the coverage metric, we take the cost-function to be the first time-derivative of $\Phi(\tau)$ at the end of the horizon i.e.,

$$C(t,\Delta t) = \dot{\Phi}(t+\Delta t) = \sum_K\Lambda_kS_k(t+\Delta t)\dot{S}_k(t+\Delta t). \tag{23}$$

Once we obtain the necessary conditions in terms of the two point boundary value problem, we can derive the feedback law in the limit as the receding horizon Δt goes to zero. As described in Appendix A, the feedback law takes the form

$$\begin{aligned} u_j(t) &= -u_{max}\frac{B_j}{\|B_j(t)\|_2}, \\ \text{where } B_j(t) &= \sum_k\Lambda_kS_k(t)\nabla f_k(x_j(t)). \end{aligned} \tag{24}$$

This feedback law is such that it makes the second time-derivative of $\Phi(t)$ as negative as possible. We note that the

controls $u_j(t)$ have no direct influence on the first time-derivative $\dot{\phi}(t)$ and it may not be possible to make $\dot{\phi}(t)$ negative. For the second-order sensor dynamics,

$$\ddot{x}_j(t) = u_j(t), \tag{25}$$

we take the cost to be of the form

$$\begin{aligned} C(t,\Delta t) &= \dot{\Phi}(t+\Delta t) + \frac{c}{2}\int_t^{t+\Delta t}\sum_{j=1}^{N} v_j(\tau)\cdot v_j(\tau)d\tau \\ &= \sum_K \Lambda_k S_k(t+\Delta t)\dot{S}_k(t+\Delta t) \\ &+ \frac{c}{2}\int_t^{t+\Delta t}\sum_{j=1}^{N} v_j(\tau)\cdot v_j(\tau). \end{aligned} \tag{26}$$

where, the additional term accounts for the time-integral of the kinetic energy of the sensors. The parameter c determines how much the kinetic energy is penalized relative to coverage. Using a similar receding horizon approach, as described for the first-order sensor dynamics above, we obtain the feedback law as

$$\begin{aligned} u_j^*(t) &= -F_{max}\frac{(cv_j(t)+B_j(t))}{\|cv_j(t)+B_j(t)\|_2}, \\ \text{where } B_j(t) &= \left[\sum_K \Lambda_k S_k(t)\nabla f_k(x_j(t))\right]. \end{aligned} \tag{27}$$

IV. DSMC WITH STOCHASTIC TARGET DYNAMICS

Let the target dynamics evolve according to a stochastic differential equation [14],

$$dz(t) = v(z(t),t)dt + b(z(t),t)d\beta(t,\omega)dt. \tag{28}$$

where, $\beta(t,\omega):\mathbb{R}\times\Omega\to\mathbb{R}$ is the standard Brownian motion. Here $(\Omega,\mathscr{A},\mathscr{P})$ is probability space whose event space is Ω, and is equipped with $\sigma-$ algebra $\mathscr{A}$ and a probability measure $\mathscr{P}$. The corresponding transformation that describes the evolution of the target can be represented as

$$z(t_f) = T(z(t_0),t_0,t_f,\omega), \tag{29}$$

which is parameterized by the realization ω. Hence, we have a tube set (7) corresponding to each realization of the ω. The average value of the fraction of time spent in these tube sets is given as an expectation. i.e.

$$d^t(x,r) = \mathbb{E}_{\mathscr{P}}\left[\frac{1}{Nt}\sum_{j=1}^{N}\int_0^t \chi_{B(x,r)}\left(T(x_j(\tau),\tau,t,\omega)\right)d\tau\right]. \tag{30}$$

Consider the family of stochastic Perron-Frobenius operators (see [15]) corresponding to the transformations $T(z(t_0),t_0,t_f,\omega)$, which is given as

$$\int_A [P^{t_0,t_f}]\nu(t_0,y)dy = \mathbb{E}_{\mathscr{P}}\left[\int_U \nu(t_0,y).\chi_A\left(T(y,t_0,t_f,\omega)\right)dy\right]. \tag{31}$$

Just as the case for deterministic dynamics, the fraction $d^t(x,r)$ is given as a spherical integral of the coverage distribution as defined in (11) i.e.,

$$\begin{aligned} d^t(x,r) &= \int_{B(x,r)} C^t(y)dy = \int_{B(x,r)}\left[\frac{1}{Nt}\sum_{j=1}^{N}\int_0^t P^{\tau,t}\delta_{x_j(\tau)}(y)d\tau\right]dy \\ &= \frac{1}{Nt}\sum_{j=1}^{N}\int_0^t\left[\int_{B(x,r)} P^{\tau,t}\delta_{x_j(\tau)}(y)dy\right]d\tau \\ &= \frac{1}{Nt}\sum_{j=1}^{N}\int_0^t \mathbb{E}_{\mathscr{P}}\left[\int_U \delta_{x_j(\tau)}(y).\chi_{B(x,r)}\left(T(y,\tau,t,\omega)\right)dy\right]d\tau \\ &= \mathbb{E}_{\mathscr{P}}\left[\frac{1}{Nt}\sum_{j=1}^{N}\int_0^t \chi_{B(x,r)}\left(T(x_j(\tau),\tau,t,\omega)\right)d\tau\right]. \end{aligned} \tag{32}$$

Just as described in the previous sections, we can use the Sobolev space distance between $C^t(.)$ and $\nu(,t)$ as a metric for coverage and design the feedback control.

V. EXAMPLES WITH FIRST ORDER SENSOR DYNAMICS

In this section we consider two examples involving coverage of moving targets, one with known and the other with uncertain dynamics. We assume that the sensor dynamics is first order in both the cases.

A. Deterministic target dynamics

In the first example, we take the target motion to be deterministic, such that it moves towards a central point with a known fixed speed. The initial uncertainty in the target position is uniformly distributed in a ring of finite size centered around the origin. The target dynamics is given as:

$$\dot{z} = v_{max}\frac{(z_c - z)}{\|z_c - z\|_2}, \tag{33}$$

v_{max} is the constant speed of the target and z_c is the central location towards which the target is moving. For this example, we use the metric as defined in (14). The feedback law as described in (24) is used and the resulting dynamics can be seen in Figure 2. The decay of the coverage metric $E^2(t)$ with time can be seen in Figure 3.

B. Uncertain target dynamics: DSMC coupled with a Kalman filter

Consider M identical targets moving independently of each other in $\mathbb{R}^2$ with uncertain dynamics. We assume that the sensors can observe the targets when they fall within their sensing range. In order to incorporate observation dynamics, it is natural to represent the target dynamics in discrete time as:

$$z_h^i = Fz_{h-1}^i + G\mathbf{w}_h, \tag{34}$$

where, $i = 1,\cdots,M$, $z_h^i = z^i(t_h)\in\mathbb{R}^n$ is the $i-$th target state at time t_h, $\mathbf{w}_h\in\mathbb{R}^n$ is process noise which is assumed to be drawn from a zero mean multivariate normal distribution

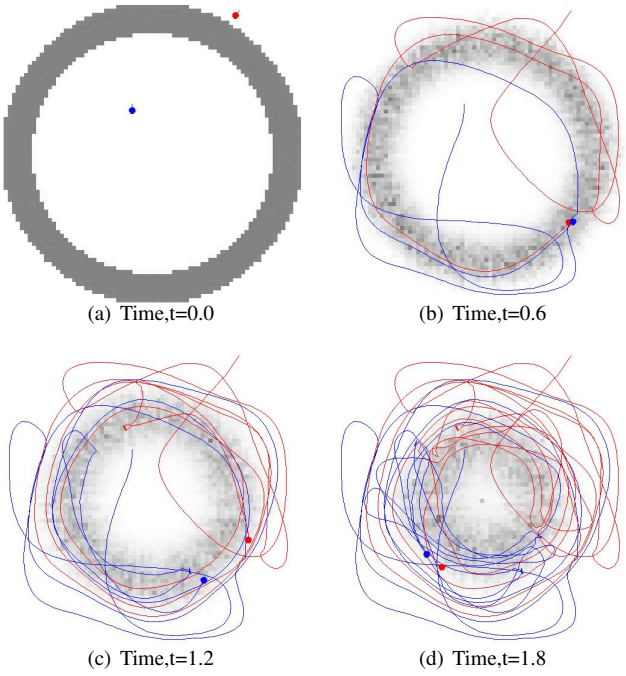

(a) Time,t=0.0 (b) Time,t=0.6

(c) Time,t=1.2 (d) Time,t=1.8

Fig. 2. Snapshots at various times of the sensor trajectories generated by the DSMC algorithm with first-order dynamics. The dynamics of the target is such that it moves toward a central point with a constant speed. The initial prior probability distribution is a uniform distribution on a ring of finite width. The grey blob in the pictures above represent the evolving uncertainty in the position of the moving target.

with covariance Q_h, i.e $\mathbf{w} \sim \mathcal{N}(0, Q_h)$. When the target is observed, the observation follows the model:

$$y_h^i = Hz_h^i + \mathbf{v}_h, \tag{35}$$

where, $\mathbf{v}_h$ is the observation noise which is assumed to be zero mean Gaussian white noise with covariance R_h, i.e. $\mathbf{v}_h \sim \mathcal{N}(0, R_h)$. Given the linear dynamics with additive white Gaussian noise and appropriate independence assumptions, the conditional probability density evolves as a multivariate Gaussian [16], i.e.

$$z_h^i \sim \mathcal{N}(z_{h|h}^i, P_{h|h}^i), \tag{36}$$

where, $z_{h|h}^i$ is the state mean and $P_{h|h}^i$ is its covariance. When the $i-$th target is observed, the state prediction and covariance update equations are given by the standard Kalman equations ([16])

$$\begin{aligned}
z_{h|(h-1)}^i &= Fz_{(h-1)|(h-1)}^i, \\
P_{h|(h-1)}^i &= FP_{(h-1)|(h-1)}^i(F)^T + GQ_h(G)^T, \\
K_h^i &= P_{h|(h-1)}^i H^T (HP_{h|(h-1)}^i H^T + R_h)^{-1}, \\
P_{h|h}^i &= (\mathscr{I}_{n\times n} - K_h^i H)P_{h|(h-1)}^i, \\
z_{h|h}^i &= z_{h|(h-1)}^i + K_h^i(y_h^i - Hz_{h|(h-1)}^i),
\end{aligned}$$

where, the superscript T denotes the transpose and $\mathscr{I}_{n\times n}$ is a $n\times n$ identity matrix. When the $i-$th target is not observed, the update equations comprises only of the prediction step, i.e.

$$\begin{aligned}
z_{h|h}^i &= Fz_{(h-1)|(h-1)}^i, \\
P_{h|h}^i &= FP_{(h-1)|(h-1)}^i(F)^T + GQ_h(G)^T.
\end{aligned}$$

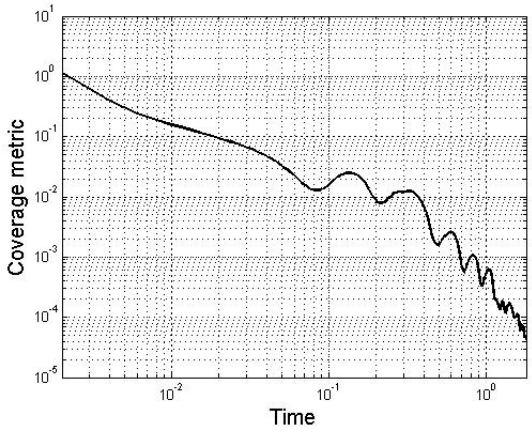

Fig. 3. Decay of the coverage metric $E^2(t)$ with time on a log-log scale for the example in Section V-A

We shall denote by $z_{0|0}^i$ and $P_{0|0}^i$, the mean and covariance, respectively associated with the initial prior. The initial prior

$$\mu_0^i(x) = \mathscr{G}(x; z_{0|0}^i, P_{0|0}^i), \tag{37}$$

evolves based on the observation process as described above such that

$$\mu_h^i(x) = \mathscr{G}(x; z_{h|h}^i, P_{h|h}^i), \tag{38}$$

where, $\mathscr{G}(x;\bar{x},\Sigma)$ is a multivariate Gaussian with mean $\bar{x}$ and covariance matrix Σ. In order to design coverage dynamics so that the sensor spends more time in regions where there is higher uncertainty in the target position, we take v in the search metric (15) to be

$$v(t_h, x) = \sum_{i=1}^{M} \mathscr{F}(\mu_h^i(x)) / \int_U \sum_{i=1}^{M} \mathscr{F}(\mu_h^i(x))dx \tag{39}$$

where $\mathscr{F}$ is defined in (17). Note that in regions where there is either very low or very high probability of finding the target, $v(t_h,x)$ assumes lower values; hence sensors do not spend much time there, and are driven in regions where the target position uncertainty is higher. The DSMC algorithm couples with the Kalman filter by using the probability distribution (39), to compute the feedback law in (24).

For simulation study we assume all targets follow first order dynamics (34), with z_k^i being the position vector in R^2, $F = \mathscr{I}_{2\times 2} + A\Delta T$, $A = diag\{a,a\}$, $G = \mathscr{I}_{2\times 2}\Delta T$, and ΔT is the sampling time. We take $M = 10$ targets with $a = 0.0015$, $G = 0.2\mathscr{I}_{2\times 2}, i = 1\cdots,10$. The targets have different initial positions and exhibit diverging dynamics. The initial target position uncertainty is a Gaussian, and evolves forward in time according to the Kalman filter Eqs. (37) or Eqs. (37), depending on whether or not the target is observed by any of the sensors. We consider $N = 2$ sensors

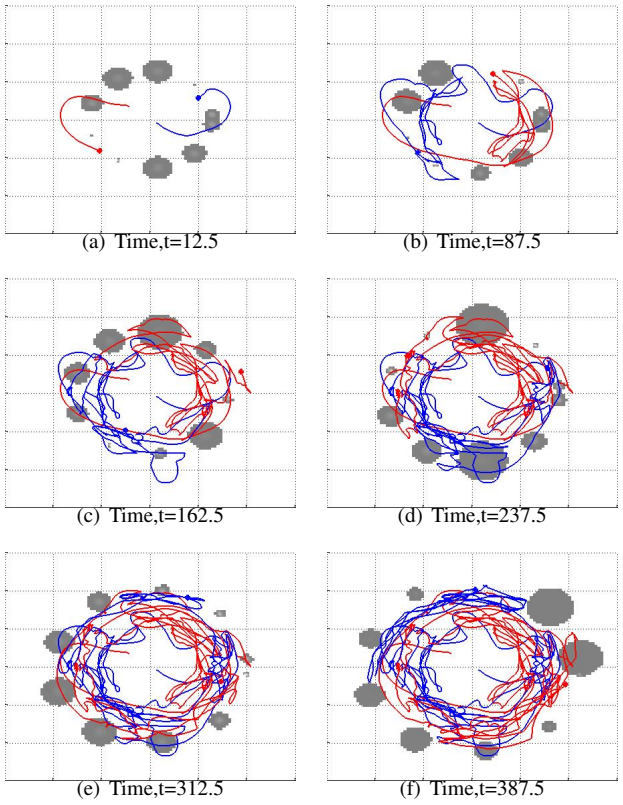

Fig. 4. Snapshots at various times of the evolving target position uncertainty (grey blobs), and sensor trajectories (red and blue curves) generated by the DSMC algorithm with first-order dynamics. The targets have diverging dynamics. The initial target position uncertainty for each target is a Gaussian, and evolves forward in time according to the Kalman filter.

with a sensing range of 10 meters, and assume that the sensors can directly measure the position of target so that $H = \mathscr{I}_{2\times 2}$ with a measurement noise covariance of $0.1\mathscr{I}_{2\times 2}$. We take the maximum sensor speed to be $u_{\max} = 5$m/sec, which corresponds roughly to be 30 orders of magnitude faster than maximum speed that targets attain.

Figure 4 shows snapshots at various times of the evolving target position uncertainty (grey blobs), and sensor trajectories (red and blue curves) generated by the DSMC algorithm with first-order dynamics. Figure 5 shows the evolution of the trace of error covariance for three targets (other targets show similar patterns). As can be seen, the trace of error covariance increases monotonically until the target is observed, at which point there is a sharp drop. Also note that the trace of error covariance remains bounded, showing that we achieve good coverage, and no target is lost. Note that the error covariance won't remain bounded forever. Since the targets are diverging, the sensors have bounded speed and the number of targets is more than the number of sensors, the estimation of the Kalman filter will diverge at some point. Our objective is just to maximize the time within which all the targets are tracked reasonably well.

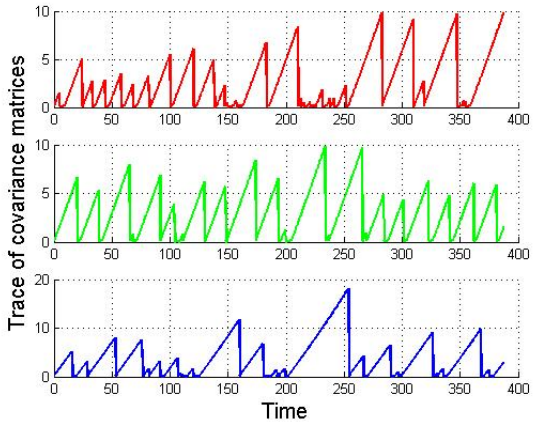

Fig. 5. Trace of error covariance for three different targets as a function of time (all the targets show similar patterns). The trace of the error covariance increases monotonically until the target is observed, at which point there is a sharp drop. The trace of the error covariance remains bounded showing that we achieve good coverage and no target is lost.

VI. Conclusions

In this paper we have extended the coverage metric introduced in [11] and [12] to a dynamic setting where the initial target prior evolves over time. The metric captures the discrepancy between the distribution of points visited by the mobile sensors when evolved forward in time according to the target dynamics with the time dependent target distribution. Using this metric, we derived centralized feedback control laws for the mobile sensors with first and second order dynamics, so that they can achieve uniform coverage of the moving target distribution with known target dynamics. We also extended this to the case when the target dynamics is uncertain. Various numerical simulations have demonstrated the effectiveness of the algorithm. These examples were restricted to the case where target motion can be described by first order dynamics, and all targets follow same motion model.

Proving convergence and limitations of the DSMC algorithm is an open and challenging problem. In particular, it is of interest to know what assumptions on the target motion are required so that the coverage metric converges to zero. In the future it is also desirable to extend the DSMC framework to deal with higher order target dynamics, to account for heterogeneity in their dynamics and incorporate target prioritization in the coverage metric. Taking into account a longer time horizon while deriving the feedback law and modifications of the algorithm to achieve decentralization in the case when there is limited communication between agents are some other possible directions to pursue in the future.

VII. Acknowledgements

The funding provided by United Technologies Research Center and the Office of Naval Research (Grant No. N00014-07-1-0587) for this work is greatly appreciated. Authors would like to thank Andrzej Banaszuk, Harshad Sane and

Thomas Frewen at UTRC and Vladimir Fonoberov of Aimdyn Inc., Santa Barbara for fruitful discussions and feedback on this work.

APPENDIX

A. Feedback control design

For convenience, let us define the following quantities

$$\begin{aligned} D^t &= NtC^t, \\ \Phi(t) &= \frac{1}{2}N^2t^2\phi^2(t) = \frac{1}{2}\sum_K \Lambda_k |S_k(t)|^2 \\ \text{where } S_k(t) &= C_k(t) - M_k(t), \\ C_k(t) &= Ntc_k(t) \text{ and } M_k(t) = Nt\nu_k(t). \end{aligned} \tag{40}$$

Note that $C_k(t)$ is given as

$$\begin{aligned} C_k(t) &= \left\langle D^t, f_k \right\rangle = \left\langle \sum_{j=1}^N \int_0^t P^{\tau,t}\delta_{x_j(\tau)}(.)d\tau, f_k(.) \right\rangle \\ &= \sum_{j=1}^N \int_0^t \left\langle P^{\tau,t}\delta_{x_j(\tau)}(.), f_k(.) \right\rangle d\tau \\ &= \sum_{j=1}^N \int_0^t \left\langle \delta_{x_j(\tau)}(.), K^{\tau,t} f_k(.) \right\rangle d\tau, \end{aligned} \tag{41}$$

where $K^{\tau,t} = [P^{\tau,t}]^*$ is the adjoint of the Perron-Frobenius operator $P^{\tau,t}$ (see [15] for details). It is well known that the adjoint of the Perron-Frobenius operator is the Koopman operator given as

$$K^{\tau,t} f_k(y) = f_k(T(y,\tau,t)). \tag{42}$$

Thus, we have

$$\begin{aligned} C_k(t) &= \sum_{j=1}^N \int_0^t \left\langle \delta_{x_j(\tau)}(.), f_k(T(.,\tau,t)) \right\rangle d\tau \\ &= \sum_{j=1}^N \int_0^t f_k(T(x_j(\tau),\tau,t))d\tau. \end{aligned} \tag{43}$$

The first time-derivative of $C_k(t)$ is given as

$$\begin{aligned} \dot{C}_k(t) &= \sum_{j=1}^N \int_0^t \frac{\partial}{\partial t} f_k(T(x_j(\tau),\tau,t))d\tau + \sum_{j=1}^N f_k(x_j(t)) \\ &= \sum_{j=1}^N \int_0^t \nabla f_k(T(x_j(\tau),\tau,t)) \cdot v(T(x_j(\tau),\tau,t),t)d\tau \\ &\quad + \sum_{j=1}^N f_k(x_j(t)). \end{aligned} \tag{44}$$

Now, the second time-derivative of $C_k(t)$ is given as

$$\begin{aligned} \ddot{C}_k(t) &= \sum_{j=1}^N \int_0^t \frac{\partial}{\partial t} \nabla f_k(T(x_j(\tau),\tau,t)) \cdot v(T(x_j(\tau),\tau,t),t)d\tau \\ &\quad + \sum_{j=1}^N \nabla f_k(x_j(t)) \cdot v(x_j(t),t) + \sum_{j=1}^N \nabla f_k(x_j(t)) \cdot u_j(t). \end{aligned} \tag{45}$$

Note that the second time-derivative of $\Phi(t)$ is given as

$$\begin{aligned} \ddot{\Phi}(t) &= \sum_K \Lambda_k \left(\dot{S}_k(t)\right)^2 + \sum_K \Lambda_k S_k(t)\ddot{S}_k(t) \\ &= \sum_K \Lambda_k \left(\dot{C}_k(t) - \dot{M}_k(t)\right)^2 + \sum_K \Lambda_k S_k(t)\left(\ddot{C}_k(t) - \ddot{M}_k(t)\right) \end{aligned} \tag{46}$$

After we plug in the expressions for $\dot{C}_k(t)$ and $\ddot{C}_k(t)$ in the above expression, we shall see that the only term influenced by the controls $u_j(t)$ is

$$\begin{aligned} U(t) &= \sum_K \Lambda_k S_k(t) \left[\sum_{j=1}^N \nabla f(x_j(t) \cdot u_j(t)\right] \\ &= \sum_{j=1}^N B_j(t) \cdot u_j(t) \\ \text{where } B_j(t) &= \sum_K \Lambda_k S_k(t) \nabla f(x_j(t)). \end{aligned} \tag{47}$$

Thus, the controls $u_j(t)$ that makes $\ddot{\Phi}(t)$ (or $U(t)$) as negative as possible is

$$u_j(t) = -u_{max}\frac{B_j(t)}{\|B_j(t)\|_2}. \tag{48}$$

B. Numerical computation of the coverage distribution

Consider the distribution without the time-averaging given as

$$D^t(x) = NtC^t(x) = \sum_{j=1}^N \int_0^t P^{\tau,t}\delta_{x_j(\tau)}(x)d\tau. \tag{49}$$

At a given time t the distribution $D^{t+\Delta t}$ at time $t+\Delta t$ is computed as

$$\begin{aligned} D^{t+\Delta t}(x) &= \sum_{j=1}^N \int_0^{t+\Delta t} P^{\tau,t+\Delta t}\delta_{x_j(\tau)}(x)d\tau \\ &= \sum_{j=1}^N \int_0^t P^{\tau,t+\Delta t}\delta_{x_j(\tau)}(x)d\tau + \sum_{j=1}^N \int_t^{t+\Delta t} P^{\tau,t+\Delta t}\delta_{x_j(\tau)}(x)d\tau \\ &= \sum_{j=1}^N \int_0^t P^{t,t+\Delta t}P^{\tau,t}\delta_{x_j(\tau)}(x)d\tau + \sum_{j=1}^N \int_t^{t+\Delta t} P^{\tau,t+\Delta t}\delta_{x_j(\tau)}(x)d\tau \\ &= P^{t,t+\Delta t}\left[\sum_{j=1}^N \int_0^t P^{\tau,t}\delta_{x_j(\tau)}(x)d\tau\right] + \sum_{j=1}^N \int_t^{t+\Delta t} P^{\tau,t+\Delta t}\delta_{x_j(\tau)}(x)d\tau \\ &= P^{t,t+\Delta t}D^t(x) + \sum_{j=1}^N \int_t^{t+\Delta t} P^{\tau,t+\Delta t}\delta_{x_j(\tau)}(x)d\tau \end{aligned} \tag{50}$$

Assuming small Δt, the second term on the right hand side can be approximated giving

$$\begin{aligned} D^{t+\Delta t}(x) &\approx P^{t,t+\Delta t}D^t(x) + P^{t,t+\Delta t}\sum_{j=1}^N \delta_{x_j(t)}(x)\Delta t \\ &= P^{t,t+\Delta t}\left[D^t(x) + \sum_{j=1}^N \delta_{x_j(t)}(x)\Delta t\right]. \end{aligned} \tag{51}$$

Thus by approximating the Perron-Frobenius operator $P^{t,t+\Delta t}$ at each time-step, we can approximate $D^{t+\Delta t}$. The Perron-Frobenius operator $P^{t,t+\Delta t}$ is approximated as in the set-oriented numerical methods by [17].

REFERENCES

[1] E. Fiorelli, N. E. Leonard, P. Bhatta, D. A. Paley, R. Bachmayer, and D. M. Fratantoni, "Multi-auv control and adaptive sampling in monterey bay," *Oceanic Engineering, IEEE Journal of*, vol. 31, no. 4, pp. 935–948, Oct. 2006.

[2] P. Rybski, N. Papanikolopoulos, S. Stoeter, D. Krantz, K. Yesin, M. Gini, R. Voyles, D. Hougen, B. Nelson, and M. Erickson, "Enlisting rangers and scouts for reconnaissance and surveillance," *Robotics and Automation Magazine, IEEE*, vol. 7, no. 4, pp. 14–24, Dec 2000.

[3] C. A. Rabbath, C.-Y. Su, and A. Tsourdos, "Guest editorial introduction to the special issue on multivehicle systems cooperative control with application," *Control Systems Technology, IEEE Transactions on*, vol. 15, no. 4, pp. 599–600, July 2007.

[4] F. Bullo, J. Cortés, and B. Piccoli, "Special issue on control and optimization in cooperative networks," *SIAM Journal on Control and Optimization*, vol. 48, no. 1, pp. vii–vii, 2009.

[5] T. Curtin and J. Bellingham, "Guest editorial - autonomous ocean-sampling networks," *Oceanic Engineering, IEEE Journal of*, vol. 26, no. 4, pp. 421–423, Oct 2001.

[6] A. Howard, M. J. Mataric, and G. S. Sukhatme, "Mobile sensor network deployment using potential fields: A distributed, scalable solution to the area coverage problem," 2002, pp. 299–308.

[7] J. Cortes, S. Martinez, T. Karatas, and F. Bullo, "Coverage control for mobile sensing networks," *IEEE Transactions of Robotics and Automation*, vol. 20, no. 2, pp. 243–255, 2004.

[8] F. Lekien and N. E. Leonard, "Nonuniform coverage and cartograms," *SIAM Journal on Control and Optimization*, vol. 48, no. 1, pp. 351–372, 2009.

[9] N. Leonard, D. Paley, F. Lekien, R. Sepulchre, D. Fratantoni, and R. Davis, "Collective motion, sensor networks, and ocean sampling," *Proceedings of the IEEE*, vol. 95, no. 1, pp. 48–74, 2007.

[10] I. Hussein and D. Stipanović, "Effective coverage control for mobile sensor networks with guaranteed collision avoidance," *IEEE Transactions on Control Systems Technology, Special Issue on Multi-Vehicle Systems Cooperative Control with Applications*, vol. 15, no. 4, pp. 642–657, 2007.

[11] G. Mathew and I. Mezić, "Spectral multiscale coverage: A uniform coverage algorithm for mobile sensor networks," in *IEEE Conf. on Decision and Control*, Shanghai, China, Dec. 2009.

[12] G. Mathew and I. Mezic, "Metrics for ergodicity and design of ergodic dynamics for multi-agent systems," *Physica D: Nonlinear Phenomena*, 2010, accepted for publication.

[13] G. Mathew, I. Mezic, and L. Petzold, "A multiscale measure for mixing," *Physica D: Nonlinear Phenomena*, vol. 211, pp. 23–46, November 2005.

[14] J. L. Doob, *Stochastic Processes*. Wiley Classics Library, 1953.

[15] A. Lasota and M. C. Mackey, *Chaos, Fractals, and Noise*. Cambridge University Press, 1994.

[16] A. H. Jazwinski, *Stochastic Processes and Filtering Theory*. Academic Press, 1970.

[17] M. Dellnitz and O. Junge, *Set Oriented Numerical Methods for Dynamical Systems*. World Scientific, 2002, pp. 221–264.